Unclassified
SECURITY CLASSIFICATION OF THIS PAGE

(2)

REPORT DOCUMENTATION PAGE

Form Approved OMB No. 0704-0188

AD-A207 391

Field	Entry
1b. RESTRICTIVE MARKINGS	None
3. DISTRIBUTION/AVAILABILITY OF REPORT	Approved for public release; Distribution is unlimited.
2b. DECLASSIFICATION/DOWNGRADING SCHEDULE	
4. PERFORMING ORGANIZATION REPORT NUMBER(S)	JA 321:061:88
5. MONITORING ORGANIZATION REPORT NUMBER(S)	JA 321:061:88
6a. NAME OF PERFORMING ORGANIZATION	Naval Ocean Research and Development Activity
6b. OFFICE SYMBOL (If applicable)	321
7a. NAME OF MONITORING ORGANIZATION	Ocean Science Directorate Naval Ocean Research and Development Activity
6c. ADDRESS (City, State, and ZIP Code)	Stennis Space Center, MS 39529-5004
7b. ADDRESS (City, State, and ZIP Code)	Stennis Space Center, MS 39529-5004
8a. NAME OF FUNDING/SPONSORING ORGANIZATION	Space and Naval Warfare Systems Command
8b. OFFICE SYMBOL (If applicable)	PMW-141
9. PROCUREMENT INSTRUMENT IDENTIFICATION NUMBER	
8c. ADDRESS (City, State, and ZIP Code)	Washington, D.C. 20363-5100

10. SOURCE OF FUNDING NUMBERS

PROGRAM ELEMENT NO.	PROJECT NO.	TASK NO.	WORK UNIT ACCESSION NO.
63704N			DN394421

11. TITLE (Include Security Classification)
GEOSAT Altimeter Sea-Ice Mapping

12. PERSONAL AUTHOR(S)
Jeffrey D. Hawkins and Matthew Lybanon

13a. TYPE OF REPORT	13b. TIME COVERED	14. DATE OF REPORT (Year, Month, Day)	15. PAGE COUNT
Journal Article	FROM ____ TO ____	1989, April	9

16. SUPPLEMENTARY NOTATION

17. COSATI CODES

FIELD	GROUP	SUB-GROUP

18. SUBJECT TERMS (Continue on reverse if necessary and identify by block number)
Altimetry, Sea Ice, Satellite Oceanography, Remote Sensing

19. ABSTRACT (Continue on reverse if necessary and identify by block number)

"Original contains color plates: All DTIC reproductions will be in black and white"

20. DISTRIBUTION/AVAILABILITY OF ABSTRACT
☐ UNCLASSIFIED/UNLIMITED ☒ SAME AS RPT. ☐ DTIC USERS

21. ABSTRACT SECURITY CLASSIFICATION
Unclassified

22a. NAME OF RESPONSIBLE INDIVIDUAL	22b. TELEPHONE (Include Area Code)	22c. OFFICE SYMBOL
Jeffrey Hawkins	601-688-5270	321

GEOSAT Altimeter Sea-Ice Mapping

JEFFREY D. HAWKINS AND MATTHEW LYBANON

Reprinted from
IEEE JOURNAL OF OCEANIC ENGINEERING
Vol. 14, No. 2,

GEOSAT Altimeter Sea-Ice Mapping

JEFFREY D. HAWKINS AND MATTHEW LYBANON

(Invited Paper)

***Abstract*—Polar sea-ice measurements are reduced to a fraction of those required for accurate sea-ice analyses and forecasts by the harsh environment (intense cold, clouds, remoteness) encountered. This severe operational data void is now being partially filled by the U.S. Navy GEOdetic SATellite (GEOSAT) active microwave altimeter.**

The 12 March 1985 GEOSAT launch enabled satellite oceanographers to continue the earlier sea-ice monitoring shown to be feasible with the GEOS-3 and SEASAT altimeters [1]. The large difference in return signals from a 13.5 GHz pulse over water versus over sea-ice permits the generation of an ice index that responds abruptly to sea-ice edges.

Sample Arctic and Antarctic operational sea-ice index plots are shown, depicting the current effort within the Remote Sensing Branch at the Naval Ocean Research and Development Activity (NORDA). This NORDA program provides graphical ice-index displays along GEOSAT nadir tracks to the Navy/National Oceanic and Atmospheric Administration (NOAA) Joint Ice Center (JIC) for assimilation into their sea-ice data bases. The altimeter's all-weather capability has been an important addition to the JIC data bases, since cloud cover can drastically curtail visible and infrared viewing, and passive microwave data has coarser resolution.

Ongoing research efforts are aimed at extracting additional sea-ice parameters from the altimeter waveform data, which contain information on the reflecting surface. Possibilities include discrimination between water, land, ice, combination water/ice, and water/land, as well as distinguishing various ice concentrations and possibly ice types. Coincident airborne passive microwave and synthetic aperture radar (SAR) data have been collected to test several methods which appear to be promising.

***Keywords*—sea ice, satellite altimetry, remote sensing, GEOSAT.**

I. Introduction

THE TASK encompassed in accurately mapping sea-ice characteristics has always suffered from a critical lack of observational data. The polar regions are severely undersampled by planes on routine patrol. Those patrols are supplemented only by a few point source reports from ships and drifting buoys. Thus, overcoming the data base shortage is obviously a satellite remote-sensing problem since large domains can be affordably scanned at reasonable spatial and temporal resolutions.

Satellite visible and infrared (IR) imagery have been hand-analyzed for years by operational ice analysts. Excellent results are possible in cloud-free scenes, but such conditions do not normally persist for the desired time frame. Wintertime and spring Arctic imagery can provide excellent viewing opportunities in many regions, but summertime photos are typically quite poor because cloudiness increases markedly and therefore dramatically limits cloud-free zones within images.

Passive microwave data have been used to partially alleviate this cloud problem, with more success noted for ice-concentration values. However, the coarse resolution (50 km with Nimbus-7 data), trouble with ice-type classification and retrievals during melt and freeze periods, and problems with atmospheric storm contamination have left holes in the sea-ice data base. All three areas of difficulty are under review with the newer Special Sensor Microwave/Imager (SSM/1) data.

It has been demonstrated that active microwave radar altimeter data from SEASAT and GEOS-3 can be used to retrieve sea-ice characteristics and thus partially fill data bases. Dwyer and Godin [1] obtained good results by taking advantage of the huge signal change that occurs when the altimeter's field of view traverses from open water to sea ice (i.e., ice edge). Validation efforts in the Bering Sea went quite well but did not extend to other areas and seasons because of the spotty nature of the GEOS-3 data and the premature failure of SEASAT.

The Navy recognized this verification shortfall when they identified a secondary mission for the U.S. Navy GEOdetic SATellite (GEOSAT) program centering on the altimeter's oceanograhic measuring capabilities. This paper will detail the efforts to use GEOSAT data to refine an ice index that is applicable to widely varying ice conditions. The following sections will detail more fully the sea-ice mapping requirements, the present Navy ice-index operational utilization, and ongoing and future work that promises to provide additional sea-ice measurement capabilities.

II. Joint Ice Center

The Joint Ice Center (JIC) at Suitland, Maryland, is a combined Navy and National Oceanic and Atmospheric Administration (NOAA) effort begun in 1976. Its duties are to map the ice edge, concentration, and type throughout both the Arctic and Antarctic Oceans as well as the Great Lakes, and to provide advance sea-ice forecasts. This joint effort permits both civilian and military agencies to plan for safer operations within this environmentally hostile region and combine severely limited resources.

The Naval Polar Oceanography Center (NPOC) represents the Navy's portion within this cooperative team. NPOC is responsible for satisfying the operational Department of Defense (DoD) polar sea-ice analysis and forecasting needs [2]. This function must be done by combining a variety of data sources in order to generate a host of products.

Fig. 1 is just one example of the many JIC Arctic sea-ice

Manuscript received May 1, 1988; revised September 20, 1988. This work was supported by the Satellite Applications and Technology (SAT) Program of the NORDA Remote Sensing Branch's Applications Development Section by Chief of Naval Operations, CNO-OP-96, under Program Element 63708N. This is NORDA contribution no. 321:061:88.

The authors are with the Remote Sensing Branch, Naval Ocean Research and Development Activity, Stennis Space Center, MS 39529-5004.

IEEE Log Number 8825748.

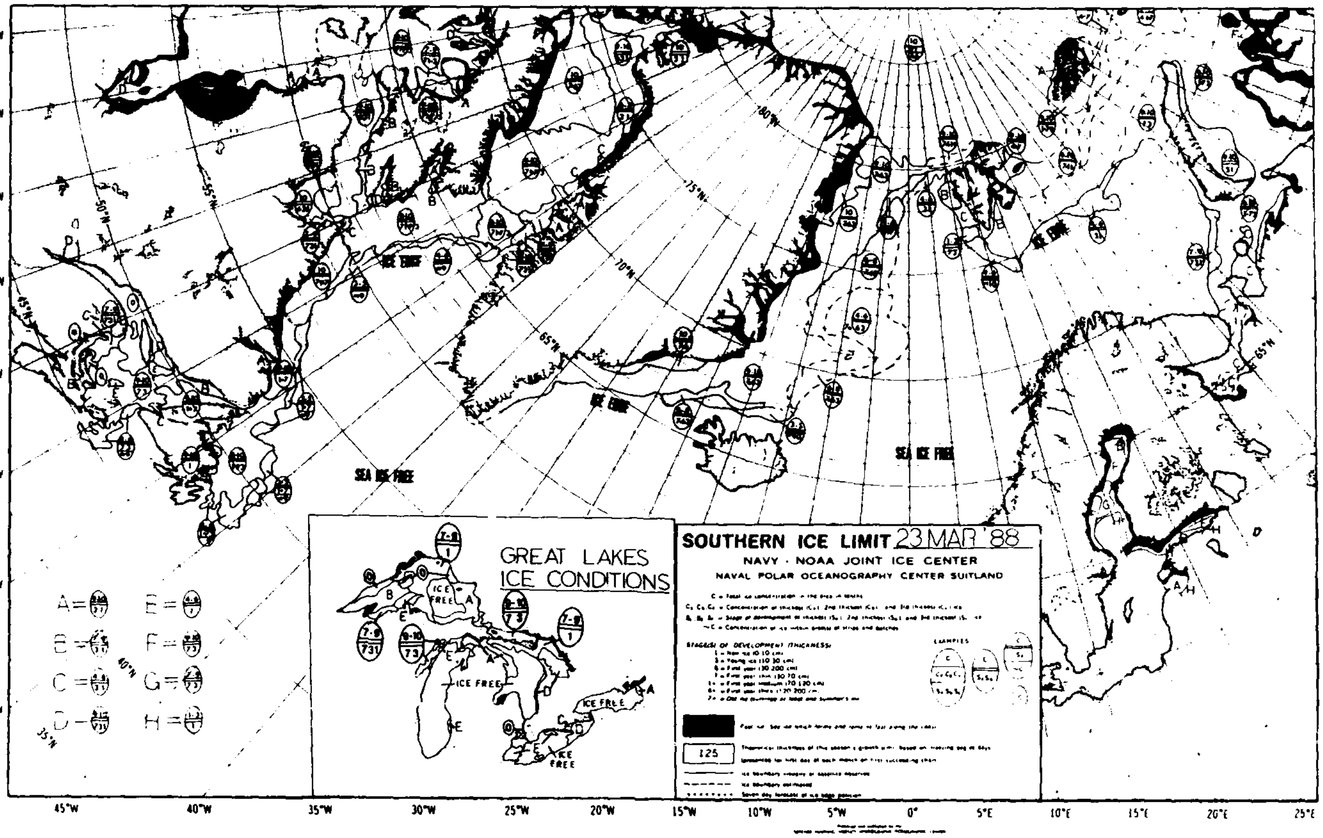

Fig. 1. Typical JIC eastern Arctic sea-ice chart depicting the ice edge, concentration, and type of ice within the region. (Note: *Dashed lines represent estimates due to lack of reliable data.*)

TABLE I
SEA-ICE DATA SOURCES

Sensor	*Type*	*Swath* (km)	*Resolution* (km)	*Revisit* times/day	*Advantage*	*Disadvantage*
			Satellite Sensors			
AVHRR	passive VIS & IR	2500	1–4	2–12	large swath	clouds
OLS	passive VIS & IR	2900	0.6–3	2–12	large swath	clouds
SMMR	passive microwave	750	50–60	0–2	penetrates clouds	small swath resolution melt ponds
SSM/I	passive microwave	1400	25–35	2–4	penetrates clouds	resolution melt ponds
			Other data			
Recon	aircraft					
	SLAR	1–10	<0.1	poor	high res.	small area
	Observer	1–15	<0.1	poor	high res.	small area
Ship	Observer	N/A	<0.1	poor	high res.	small area
Buoy		N/A	point source	poor	inexpensive	point source

products. The ice edge in the eastern Arctic is delineated throughout the area, and ice concentration and type are noted using the International Egg Code nomenclature [3]. Note that dashed lines represent estimates due to lack of reliable data. This chart covers half the Arctic basin and is updated once per week.

To map sea ice over such vast, remote regions, the JIC relies heavily on polar-orbiting environmental satellites because of their large spatial swaths and frequent repeat-times each day. However, each data platform/sensor has a number of advantages and disadvantages which either enhance or limit its contributions to the total sea-ice data base. Table I outlines the major sea-ice data sources available to the ice analysts and illustrates the major factors associated with each one.

Visible and IR imagery from the NOAA Advanced Very High Resolution Radiometer (AVHRR) and Defense Meteorological Satellite Program (DMSP) Operational Line Scanner (OLS) have long been the cornerstones of the JIC data bases. The continuous effort to keep these families of satellites operationally available (i.e., NOAA-5, -6, -7, -8, -9, -10, -11, and DMSP F-5, -6, -7, -8, -9) has provided the long-term access required to satisfy many ice mapping needs. Both the AVHRR and OLS offer very good spatial resolution and excellent swath coverage, but these benefits have been limited because all imagery is analyzed in hardcopy (not digital) form. This limitation will be rectified when the JIC receives its digital ice forecast and analysis system (DIFAS) in January, 1989.

Hardcopy imagery, used extensively by trained ice analysts to detect sea-ice conditions throughout the polar regions, provides excellent data when the images are cloud-free. However, persistent cloud cover can rapidly render this data type useless over varying periods and thus negate the fine resolution. It should be noted that many instances occur when the open-water areas near the ice edge are obscured by clouds while the sea ice itself is cloud-free and readily viewed.

Passive microwave satellite data (Table I) have been used for many years to penetrate cloudy atmospheric conditions and permit "all-weather" sensing of polar sea ice. The Nimbus Electrically Scanning Microwave Radiometer (ESMR) and Scanning Multichannel Microwave Radiometer (SMMR) have for many years significantly enhanced the JIC sea-ice mapping capabilities, but their poor spatial resolution has been a persistent problem [4], [5]. The problem is especially severe for ice edge, polynya, and near-shore sea-ice mapping where resolution is critical.

Problems with the geophysical algorithms applied to the passive microwave data have also prevented ESMR and SMMR data from realizing their potential. Heavy rain and winds have earlier contaminated sea-ice retrievals, but vigorous efforts using multiple channels indicate that significant progress has been made. While ice concentration algorithms have done quite well, efforts to discriminate between first-year and multi-year ice have met with only partial success [6]. These limitations will be improved upon greatly when the SSM/I uses validated operational algorithms.

A variety of other data sources such as drifting buoys, airborne reconnaissance with ice observers and sensors, ships, and data from other countries round out the available information used to generate sea-ice maps. However, even after incorporating all these data sources, gaps still remain in our ability to map present conditions (nowcasts), thus affecting the initial conditions for forecasts via numerical models.

III. GEOSAT Ocean Applications Program

GEOSAT's primary mission was to provide the dense global grid of altimeter data required to improve the determining of the earth's gravitational field. However, the Oceanographer of the Navy also formulated the GEOSAT Ocean Applications Program (GOAP), whose goal was to conduct an operational demonstration of the altimeter's usefulness to gather all-weather ocean environmental data. For over two years NORDA's Remote Sensing Branch has analyzed this data for GOAP [7].

Data collected by the altimeter are received by the only ground station, at the Johns Hopkins Applied Physics Laboratory (APL), and are processed into NORDA Data Records (NDR's). The NDR's, which contain sensor-corrected altimeter data, corrections for satellite and instrument errors, and orbit information, are transmitted promptly to NORDA over a 9600-baud, dedicated telecommunications circuit.

NORDA then processes this data to provide information on mesoscale ocean features, surface wind speed, significant wave height, and sea-ice edge. Arctic and Antarctic products based on the sea-ice edge are provided daily to NPOC. The altimeter's all-weather capability has helped to make these products useful, especially since cloud cover frequently renders other sensors useless.

IV. GEOSAT Altimeter

The U.S. Navy GEOSAT was built by the APL and launched on March 12, 1985. The satellite carries a single instrument, a 13.5-GHz nadir-looking pulse compression radar altimeter. It is similar to the SEASAT altimeter in its mechanical, thermal, and electrical interfaces, but includes some engineering changes intended to extend its lifetime and reduce its noise level [8]. The reflected pulses provide three basic types of information: the satellite altitude above the surface, the significant wave height, and the wind speed along the satellite track (the last two refer to returns from open water).

Fig. 2 illustrates the illumination of the surface for the case in which the surface relief is small compared to the transmitted pulse width. This figure shows the surface area illuminated at time increments equal to the duration of the transmitted pulse width and illustrates how the reflected signal received by the altimeter changes with time for the case of diffuse scattering, as from the sea surface. The mean received power, which increases linearly with time to a plateau, eventually falls off because of the finite antenna beam width and off-nadir scattering. (Increasing the surface relief, as in the case of higher waves in open ocean, increases the rise time and decreases the slope of the leading edge of the return pulse.)

The return pulses from sea ice have a significantly different shape than returns from the ocean [9], [10]. Fig. 3 illustrates that difference. Ice, unlike water, tends to produce specular reflection so that a much larger portion of the impinging

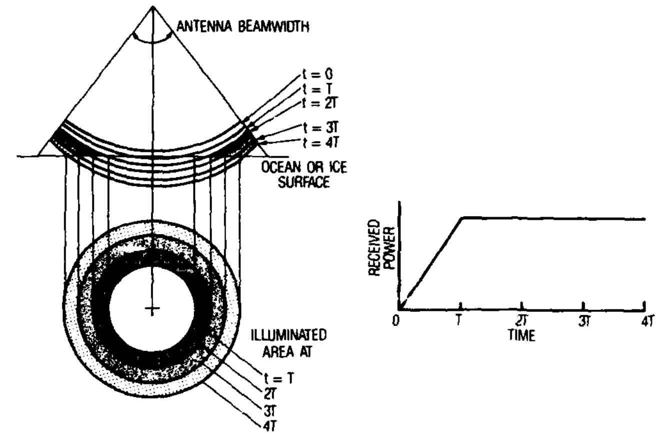

Fig. 2. Illumination of the earth's surface by an altimeter pulse of width T.

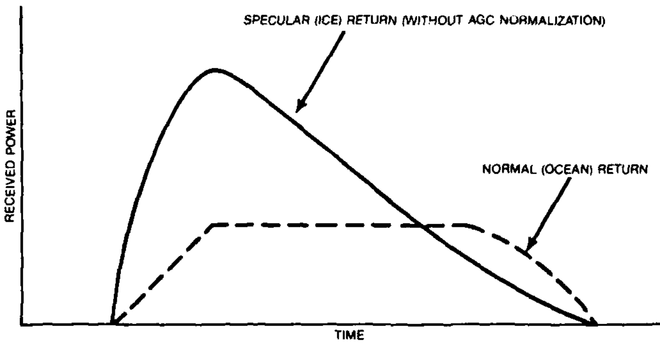

Fig. 3. Ice and ocean altimeter return waveforms.

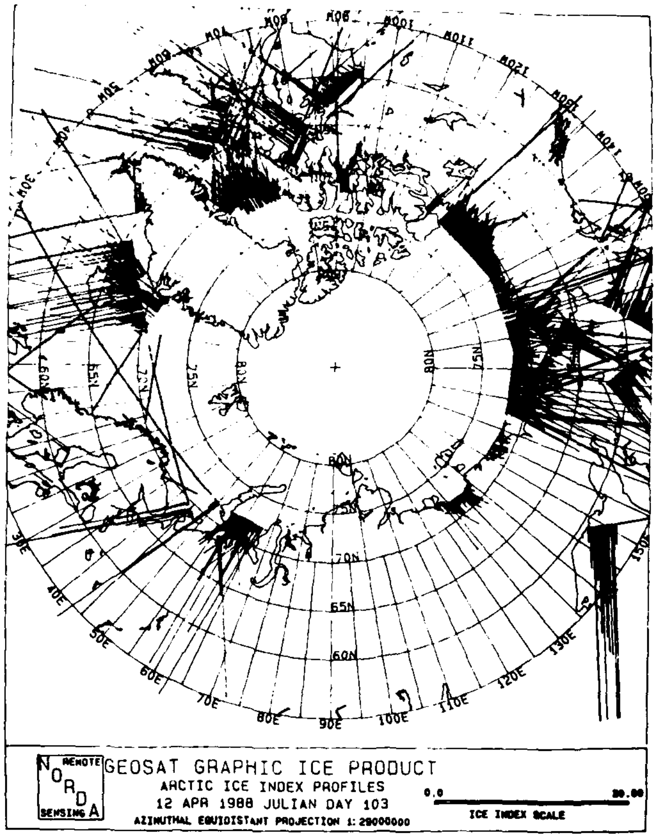

Fig. 4. Sample GEOSAT ice-index graphic product for the Arctic. Ice indexes are plotted perpendicularly to the track according to the scale in the lower-right corner. All index values < 1 have been suppressed.

energy at any angle will reflect off the ice surface at an angle equal to the angle of incidence. Thus the early return (that received from nadir) is much stronger than the latter part of the return (that received at angles off-nadir). So both the signal strength and the shape of the reflected pulse are modified. Dwyer and Godin [1] developed a semiempirical algorithm for the GEOS-3 altimeter that measures strength and shape differences. The algorithm is

$$\text{Index} = [(100 + AGC)/(100 \times AASG)] - 10 \quad (1)$$

where AGC = automatic gain control signal, and $AASG$ = average attitude/specular gate signal [1].

The Dwyer–Godin algorithm as modified for GEOSAT is

$$\text{Index} = [(100 + AGC)/(100 \times VATT)] \quad (2)$$

where

$$VATT = [(ATTG - ATTGE)/(AGCG - ATTGE)] \quad (3)$$

and the intermediate quantities are functions of the 60 basic waveform samples (the sample indexing is the same as for the SEASAT altimeter [11]): $ATTG$ = mean of last eight samples, $ATTGE$ = mean of first eight samples, and $AGCG$ = mean of center 48 samples (not including the track point gate).

$VATT$ is known as "voltage proportional to attitude" and is used in corrections for off-nadir pointing errors in the computation of several ocean parameters. The GEOSAT ice index is a number in the range 0.6 to 0.7 over water, and over ice is greater than 1. Thus, water–ice transitions are evident in the time history of the ice index.

The GEOSAT altimeter provides dense, all-weather measurements along the satellite's nadir track, but the "swath" width is only a few kilometers. The inclination of the satellite's orbit limits coverage to between 72° N and S latitudes. Within these limits, however, GEOSAT is able to provide a valuable data source that significantly increases the available sea-ice information. Ice-index values are plotted on charts made to the same scale and projection as NPOC's master working charts. These plots show ice-index profiles over water, with the satellite's nadir tracks as base lines. Figs. 4 and 5 are sample ice-index plots for the Arctic and Antarctic regions.

V. GEOSAT Coverage

GEOSAT was initially injected into an 800-km altitude, 108° inclination orbit that generated a three-day near-repeat ground track. During October, 1986, the satellite was moved into an exact repeat mission (ERM) orbit that was slightly adjusted to repeat exactly every 244 revolutions (17.05 days).

Figs. 6 and 7 depict a typical track "laydown" for one day during the ERM, which is scheduled to continue until 1991 or 1992. The Navy has funded ground operations in anticipation of a "healthy" sensor and data during this time frame. Extended operation into the 1990's would enable it to overlap with the next environmental satellite carrying an altimeter, the European Space Agency (ESA) Remote Sensing Satellite (ERS-1).

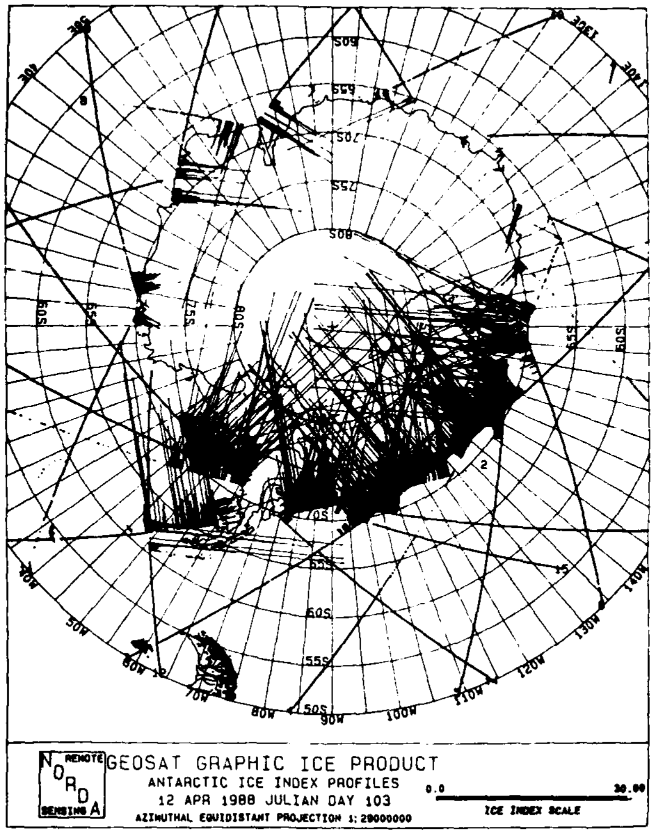

Fig. 5. Sample GEOSAT ice-index graphic product for the Antarctic.

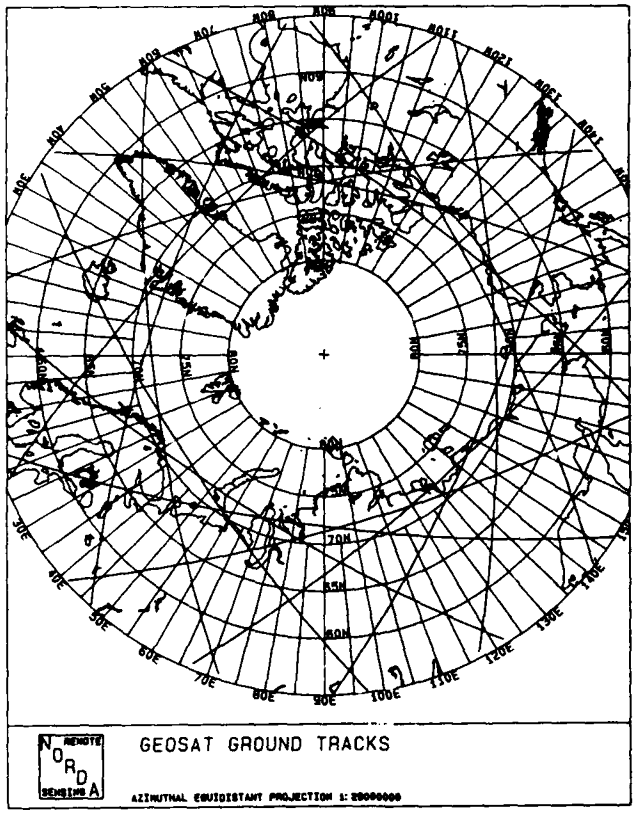

Fig. 6. One day of GEOSAT ERM ground tracks in the Arctic.

The track plots readily reveal several pluses and minuses for GEOSAT sea-ice mapping. Immediately apparent is the data void poleward of 72° latitude. The realization that the swath is the same size as the sensor footprint (2–4 km) also suggests many problems associated with temporal and spatial sampling deficiencies. It is thus clear that one single-beam altimeter is severely limited and can be counted on only to fill in data gaps.

The Navy is thus using GEOSAT data as an additional all-weather information source. Each major Arctic basin (e.g., East Greenland, Barents, Beaufort, Chukchi, Bering Sea, etc.) is sampled 3 to 4 times daily. Sampling increases dramatically near 72° as the tracks converge. This enables long passes through ice-infested waters and potentially produces numerous sea-ice data points, especially for those areas where ice motion is small and the ice analyst can use more than one day as input. Fig. 8 is a three-day Arctic track plot which shows that a wealth of data can be gathered between 65° N and 72° N as the tracks bend westward. Sea-ice mapping via GEOSAT data is thus enhanced within this section of the world.

Fig. 7 readily exhibits a different picture for Antarctic sampling. Land masses extend toward the equator from 72° S for slightly more than 50 percent of the area enclosed by this latitude band (60° S to 72° S). Such coverage, combined with the fact that the ice edge in the remaining open-water basins (Weddell and Ross Seas) is often within GEOSAT range, makes Antarctic sea-ice mapping via GEOSAT more feasible than in the Arctic. This situation is welcome, since less AVHRR data is available in the Antarctic because direct readout stations are not presently sending data to the JIC.

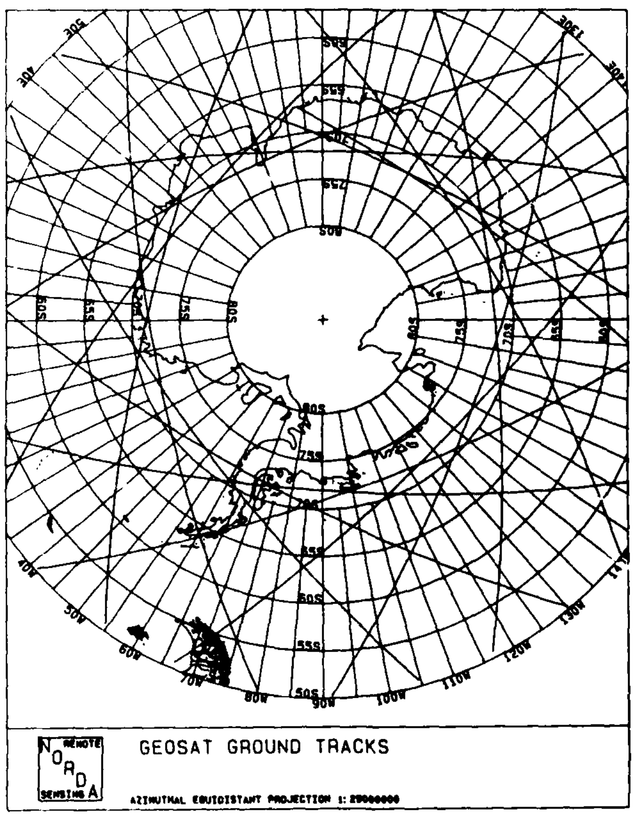

Fig. 7. One day of GEOSAT ERM ground tracks in the Antarctic.

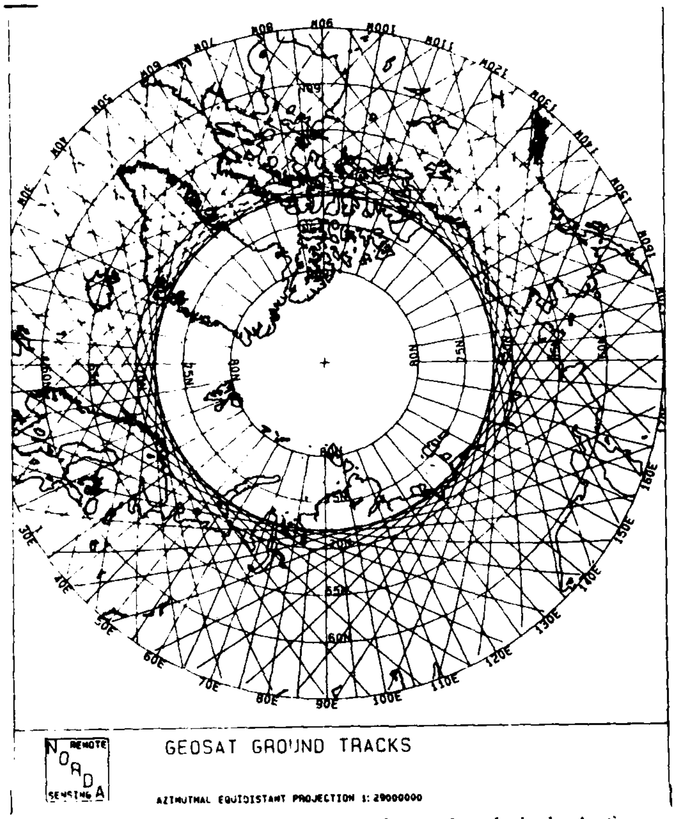

Fig. 8. Three days of GEOSAT ERM ground tracks in the Arctic.

VI. Validation

Mapping sea-ice parameters is difficult to begin with, so verifying them is an extremely arduous task at best. NORDA has enlisted a variety of spaceborne and airborne sensors to determine if GEOSAT-determined ice edges are reasonable. The verification data was obtained by using a combination of AVHRR and airborne passive and active microwave sensors.

NORDA chose NOAA AVHRR data as the prime verification tool because it has the following characteristics: A large swath, frequent repeat times and thus good temporal matchups, 1-km spatial resolution, and multispectral imaging. The majority of comparisons with GEOSAT data involved 1-km visible data in the East Greenland Sea. A more limited data set was collected in the Kara Sea and the Antarctic using 1-km IR data.

The marginal ice zone (MIZ) within the East Greenland Sea takes on a host of shapes and perturbations dependent on the combined wind and current conditions. Very accurate ice-edge boundaries can be defined when wind flow is toward the ice ("on ice"). The MIZ becomes very compact as many loose pieces and floes converge toward a new and well-defined line of demarcation between open water and sea ice. These conditions have been used as much as possible in this study in order to increase the accuracy of AVHRR ice-edge locations.

Sharp ice edges along the MIZ and the fact that numerous GEOSAT tracks cross the Greenland coast between 60° N and 72° N permit the generation of 3 to 4 ice-edge points per day, provided that the cloud conditions are favorable. Generally, in March, April, and May cloud-free viewing is at a maximum and numerous images covering large ice-edge segments are available for acquisition by NORDA's Satellite Digital Receiving and Processing System (SDRPS). SDRPS can access both Local Area Coverage (LAC—1 km) and Global Area Coverage (GAC—4 km) data.

Fig. 9 represents a typical example of the advantages and disadvantages inherent in the original NORDA GEOSAT sea-ice index. The May 10, 1987, image (AVHRR channel 2, surface reflectance) has been subsampled by two to show the ice edge from 67° N to 72° N. The resultant 2-km resolution image (512 × 512 pixels or about 1000 km on a side) contains a well-delineated MIZ extending along all but the extreme southern sections where clouds obscure the coast and the waters south and west of Iceland.

The image has been calibrated and earth located to 1-pixel accuracy using NORDA's Interactive Digital Satellite Image Processing System (IDSIPS). This set of hardware/software is based on a VAX 8300 computer and an International Imaging System (I^2S) display. The polar stereographic projection is labeled with 1° latitude and 5° longitude grid lines, while the land mask is inlaid within a graphics plane. The image has been contrast-stretched to bring out the sea-ice features, while ignoring the thin clouds in the west.

Three ascending and two descending GEOSAT tracks pass over sea ice on May 10, 1987. All ascending tracks intersect the ice edge in a near-perpendicular transect with only the southern one appearing to miss flagging the ice edge correctly, as seen by matching the AVHRR edge location with the first spike in ice-index values. Both descending tracks do quite well on the ice edge, but nonetheless illustrate a frequent problem involving data gaps (i.e., large sections have index values less than 1 or are missing for some reason).

The northernmost track readily exhibits numerous data gaps consisting of 2 to 5 data points. The absence of ice-index values causes the ice analyst confusion—should the data holes be interpreted as open-water segments or simply bad data? A similar situation is also depicted in the descending pass that grazes the MIZ and hits sea ice four separate times. The initial ice edge is marked well in some cases, but poorly in others.

NORDA undertook an effort to explain the data gaps by first looking at the parameters used to compute the ice index, AGC and VATT. These values were plotted along several tracks and quickly exposed a major problem. VATT numbers were often negative, thus causing the ice-index value to be set to zero via a data quality check. Further study revealed that the VATT value being used was not the one directly based on features of the altimeter return waveform (3). The VATT parameter has been adjusted so that tables previously prepared for use in the calculation of off-nadir angle corrections to ocean (water) parameters, based on preflight calibration, could be used without modification. The adjustment was a linear transformation: Multiplication by one constant and the addition of another. This adjustment resulted in the frequent production of negative VATT values for return pulses from ice.

NORDA (with the help of S. Laxon) proceeded to recompute the original VATT values and insert them into the sea-ice index formula (2). The results are dramatically evident in Fig. 10. All the data gaps have been eliminated and two very important facts are clear:

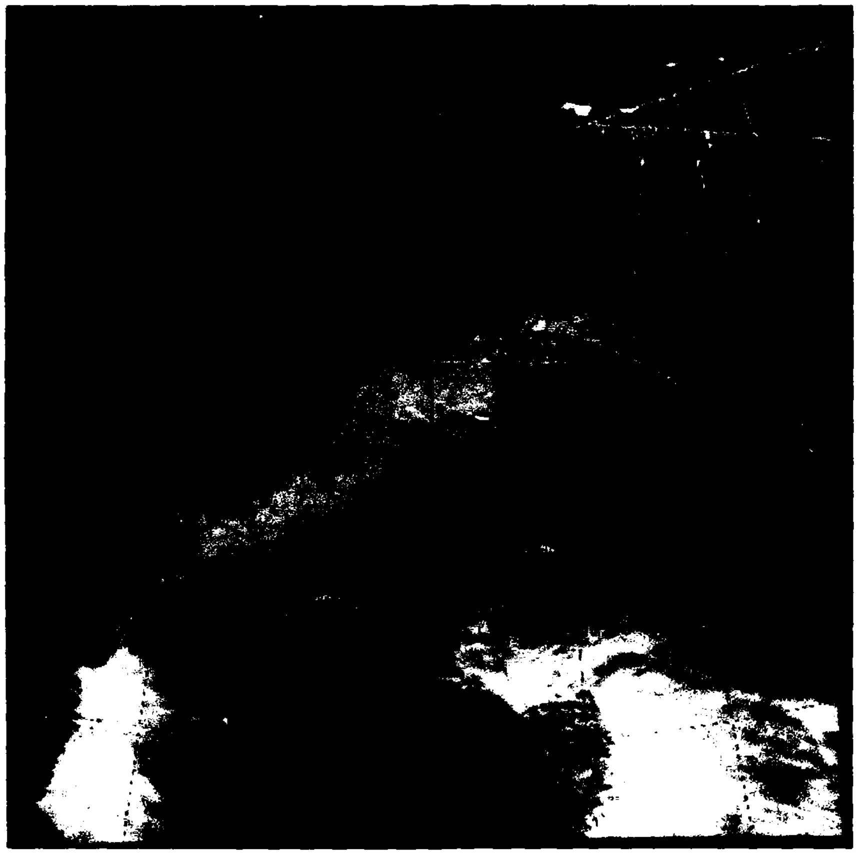

Fig. 9. AVHRR channel 2 (surface reflectance) May 10, 1987, East Greenland Sea image with the original GEOSAT ice-index superimposed. Image enhanced for sea ice.

Fig. 10. AVHRR channel 2 (surface reflectance) May 10, 1987, East Greenland Sea image with revised ice-index superimposed. Image enhanced for sea ice.

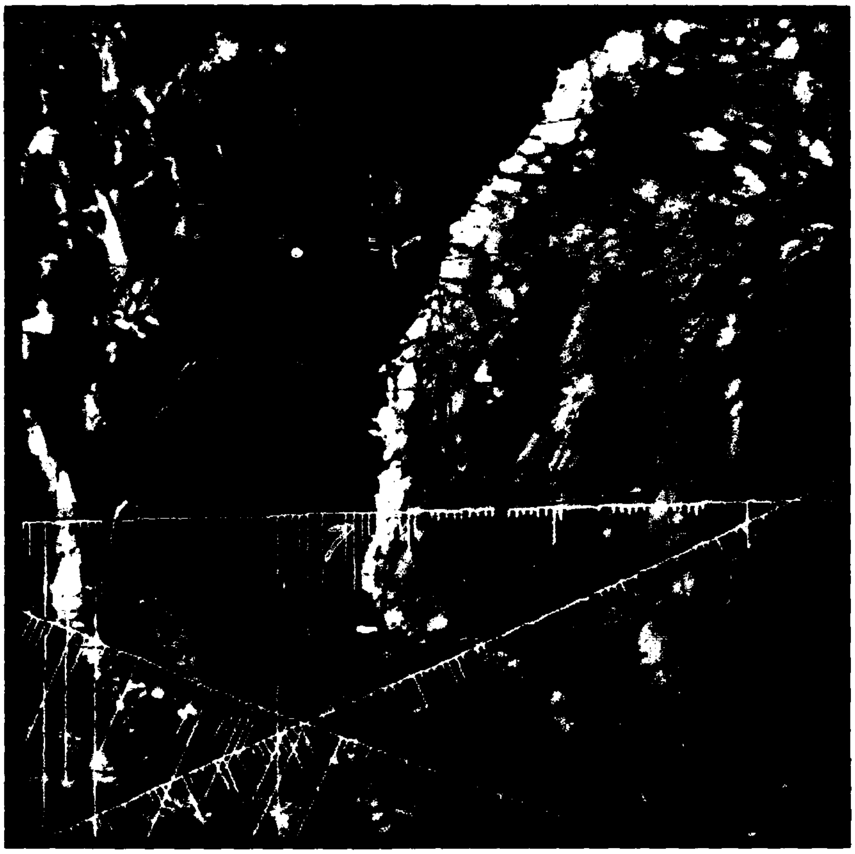

Fig. 11. AVHRR channel 4 (IR) February 21, 1986, Kara Sea image with original GEOSAT ice-index superimposed. Image enhanced to bring out sea-ice detail.

Fig. 12. AVHRR channel 4 (IR) February 21, 1986, Kara Sea image with revised ice-index superimposed. Image enhanced to bring out sea-ice detail.

1) The location of ice-edge positions has been enhanced, as is evident in the much better agreement that now exists for the southernmost track as well as the MIZ transect. The four discrete zones or perturbations eastward of the track are very accurately detected with the new sea-ice index.

2) The removal of data gaps now permits the analyst to map ice *within* the ice edge, whereas data gaps previously limited the interpretation to the edge only.

It is also quite interesting to note the high variability associated with the index values as the sensor traverses from open water, through the MIZ, into the pack ice, and then up onto the fast ice near shore. Thus, the question is whether the ice index is sensitive to ice concentration or some form of ice type manifested in characteristics such as roughness. Subsequent examples will begin to clarify this idea.

We therefore present the data collected on February 21, 1986, in the Kara Sea. Fig. 11 is a full 1-km resolution (512 × 512) infrared (AVHRR channel 4) image with three superimposed GEOSAT tracks and the accompanying original NORDA sea-ice index. The data gap problem is once again prominent and strictly limits ice-index utilization for this area. However, several other ice-index features are seen for the first time. The Kara Sea is characterized by the presence of two basic ice types. Rough first-year ice covers the largest area and is identified by the bright white (cold) IR signature with numerous leads running among it. Smooth, dark (warm), very young, thin ice is evident in the refrozen polynya to the west and in the refrozen lead located on the far right. These IR-defined ice types are reflected in the original ice index by large, highly variable values over the new ice and much smaller homogeneous values over the high-concentration first-year ice.

Fig. 12 reveals the changes made when the updated ice index is calculated. The data gap problem has been eliminated once again, but the index variability, so readily seen in the revised East Greenland Sea image (Fig. 10) and in the original Kara Sea image (Fig. 11), has been reduced considerably. There is still a factor-of-two increase in index values over the young, thin ice, with some spikes in the refrozen lead, but we have lost much of the sensitivity apparent earlier.

NORDA is presently looking into several means to optimize the combination of AGC and VATT for production of a general purpose (i.e., all regions and seasons) ice index that can be used to detect ice edges and ice types. This goal may not be feasible and an increased regional emphasis may have to be adopted.

VII. Future Work

Several opportunities exist to help answer some of the questions raised here. NORDA will continue to acquire AVHRR data periodically in both polar regions for direct comparisons with the GEOSAT sea-ice index. Extensive data sets in the Chukchi and Beaufort Seas have been collected and are nearing process completion. NORDA has also collected nine tracks of K-Band Radiometric Mapping System (KRMS, 33-GHz passive microwave) data in March, 1987, within the East Greenland Sea. This scanner underflew 3 to 4 GEOSAT tracks per day as outlined in Fig. 1. The KRMS swath allows the sensor to straddle the GEOSAT footprint (15 km at 20 000 ft, 7.5 km at 10 000 ft) while still providing very good spatial resolution [12], [13]. This data is now being processed to provide a highly accurate breakdown of ice concentration by ice type within the GEOSAT footprint.

Airborne Synthetic Aperture Radar (SAR) data from the Interra STAR 2 System [14] was also collected for five GEOSAT underflights during April, 1987, at the end of MIZEX-87 [15]. This joint effort with two NORDA programs, the ERS-1 Advanced Sensor Analysis Program and the Satellite Applications and Technology Program, acquired excellent quality high-resolution digital SAR imagery along the altimeter tracks. These transects sampled a variety of ice types and will help greatly in delineating the full potential of the sea-ice index.

Another approach that NORDA deems promising is the application of linear unmixing theory to the extraction of ice types and concentrations from altimeter waveform data. Unmixing theory has been applied for many years to a variety of geology problems [16]. Recent work in unmixing theory [17] has extended these analysis techniques into new areas such as waveform analysis. Application of this method, which treats waveforms as multivariate data vectors formed by variable combinations of pure "end members," is underway for several cases where coincident SAR, photography, passive microwave imagery, or ground truth is available. These data sets should permit a thorough evaluation of the unmixing approach to waveform analysis.

It appears likely that additional sea-ice information can be derived from the waveform data or possibly the ice index itself. Analysis of the coincident airborne data base will be the first step NORDA takes in investigating the potential expansion in applications. This field of study holds promise in increasing our utilization of the limited space platforms now in orbit or soon to be launched (ERS-1 and TOPEX will carry microwave altimeters). Cooperative efforts are encouraged, since polar data collection programs are prohibitively expensive. In this framework, NORDA is actively planning participation in ground truth and algorithm research programs for these environmental platforms.

Acknowledgment

The authors are glad to acknowledge the many contributions that made this effort possible. S. Laxon of the Mullard Space Science Laboratory (MSSL, part of University College, London) efficiently performed the work that greatly improved the GEOSAT ice-index calculation. This progress has opened up new applications. D. Eppler and D. Johnson of NORDA have provided valuable consultation during various research stages and are directly involved in ongoing and future efforts to extract additional sea-ice characteristics from altimetry. C. Johnson (NORDA) has consistently produced superior programming efforts which enabled operational status in spite of a variety of significant problems. Sverdrup Technology employees N. Koenenn and Y. Crook generated ice-index overlays, and F. Abell, Jr., processed the AVHRR imagery. T. Bogart, J. Chase, and W. Owens (Sverdrup) produced the ice-index software, while P. Phoebus (NORDA) and several reviewers considerably helped to refine the original manuscript draft. The compilation of this paper was done by the NORDA Remote Sensing Branch's Applications Development Section and was directly supported under the Satellite Applications and Technology (SAT) Program, A. E. Pressman, Program Manager.

References

[1] R. W. Dwyer and R. H. Godin, "Determining sea ice boundaries and ice roughness using GEOS-3 altimeter data," NASA Contractor Rep. 156862, 1980.

[2] H. Rosner, "The NPOC capabilities and limitations in sea ice analysis and forecasting," presented at the U.S. Navy Symp. on Arctic/Cold Weather Operational Support for Surface Ships, Naval Surface Weapons Ctr., Dalhgren, VA, Nov. 20, 1987.

[3] WMO Commission for Marine Meteorology, 4th session, working group on sea ice (Geneva), Final Rep. Oct. 25-29, 1982.

[4] D. T. Eppler, "Assessment of potential SSM/I ice products in light of ESMR and SMMR ice classification algorithms," Naval Ocean Research and Development Activity, NSTL, MS, Tech. Note 220, 1983.

[5] J. C. Comiso and H. J. Zwally, "Antarctice sea ice concentrations inferred from Nimbus 5 ESMR and Landsat imagery," *J. Geophy. Res.*, vol. 88, no. C8, pp. 5836-5844, 1982.

[6] J. C. Comiso, "Characteristics of Arctic winter sea ice from satellite multispectral microwave observations," *J. Geophys. Res.*, vol. 91, no. C1, pp. 975-994, 1986.

[7] M. Lybanon and R. L. Crout, "The NORDA GEOSAT ocean applications program," *Johns Hopkins APL Tech. Dig.*, vol. 8, pp. 212-218, Apr.-June 1987.

[8] J. L. MacArthur, P. C. Marth, Jr., and J. G. Wall, "The GEOSAT radar altimeter," *Johns Hopkins APL Tech. Dig.*, vol. 8, pp. 176-181, Apr.-June 1987.

[9] D. T. Eppler, "Possible applications of GEOSAT-A radar altimeter data to ice forecasting in polar regions," Naval Ocean Research and Development Activity, NSTL, MS, Tech. Note 177, 1982.

[10] L. M. H. Ulander, "Interpretation of SEASAT radar-altimeter data over sea ice using near-simultaneous SAR imagery," *Int. J. Remote Sensing*, vol. 8, no. 11, pp. 1679-1686, 1987.

[11] J. L. MacArthur, "SEASAT—A radar altimeter design description," The Johns Hopkins Univ., Appl. Phys. Lab., Laurel, MD, Rep. SDO-5232, 1978.

[12] D. T. Eppler, L. D. Farmer, A. W. Lohanick, and M. C. Hoover, "Classification of sea ice types with single-band (33.6 GHz) airborne passive microwave imagery," *J. Geophys. Res.*, vol. 91, no. C9, pp. 10661-10695, 1986.

[13] D. T. Eppler and J. D. Hawkins, "NORDA arctic data collection, processing, and interpretation capabilities," Naval Ocean Research and Development Activity, NSTL, MS, Rep. 129, 1985.

[14] A. D. Nichols, J. W. Wilhelm, T. W. Gaffield, D. R. Inkster, and S. K. Leung, "A SAR for real-time ice reconnaissance," *IEEE Trans. Geosci. Remote Sensing*, vol. GE-24, pp. 383-389, May 1987.

[15] D. R. Johnson and J. D. Hawkins, "The marginal ice zone experiment: MIZEX-87," *European Sci. Notes* (U.S. Office of Naval Research, London), vol. 41, no. 10, pp. 567-570, 1987.

[16] R. Ehrlich and W. E. Full, "Sorting out geology—Unmixing mixtures," in *Use and Abuse of Statistical Methods in the Earth Sciences*, W. Size, Ed. New York: Oxford Univ. Press, 1987.

[17] J. R. Chase and R. J. Holyer, "Estimation of sea-ice type and concentration by linear unmixing of GEOSAT altimeter waveforms," presented at IGARSS '88 (Edinburgh, Scotland), Sept. 13-16, 1988.

★

Jeffrey D. Hawkins received the B.S. and M.S. degrees in meteorology from the Florida State University, Tallahassee, in 1976 and 1979, respectively.

After graduation, he participated in SEASAT scatterometer validation and air-sea interaction studies near hurricanes while working for the Hurricane Research Division, AOML (Atlantic Oceanographic and Meteorological Lab. Miami, FL). In late 1980 he accepted a position as oceanographer in the Remote Sensing Branch of the Naval Ocean Reserach and Development Activity (NORDA, Stennis Space Center, MS). His present duties as Head, Applications Development Section, involve a wide variety of R&D programs aimed at utilizing spaceborne environmental sensors (AVHRR, OLS, GEOSAT altimeter, SSM/I, etc.) to meet specific Navy oceanographic requirements in the areas of sea-surface temperature, sea-surface height, and sea ice.

Mr. Hawkins is a member of the American Geophysical Union, the American Meteorological Society, the Oceanography Society, and the American Society for Photogrammetry and Remote Sensing.

★

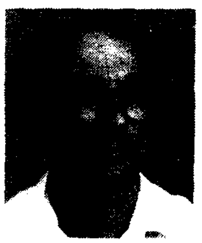

Matthew Lybanon received the B.S. and M.S. degrees in physics from the Georgia Institute of Technology, Atlanta, in 1960 and 1962, respectively.

He conducted research in remote sensing, image processing, and pattern recognition while employed by the Computer Sciences Corporation at NASA's Marshall Space Flight Center and Stennis Space Center (previously called National Space Technology Laboratories). In 1981 he joined the Naval Ocean Research and Development Activity (NORDA), Stennis Space Center, MS. A member of NORDA's Remote Sensing Branch, he has been Principal Investigator for the GEOSAT Ocean Applications Program, for a project to develop knowledge-based techniques for the automated interpretation of oceanographic satellite data, and for other work to provide analysis tools for Navy oceanographic centers. His current professional interests include artificial intelligence, image processing, generalized nonlinear least squares methods, and applications of those topics to the extraction of information on ocean dynamics and sea ice from satellite observations.

Mr. Lybanon is a member of the American Physical Society. He was awarded a NASA commendation for image-processing work to help assess the damage to Skylab's solar panels when they opened prematurely during launching.